Measurement of transmission functions in lightweight buildings for the prediction of structure-borne sound transmission from machinery

Fabian Schöpfer[1,2], Carl Hopkins[1], Andreas R. Mayr[2], Ulrich Schanda[2]
[1] Acoustics Research Unit, School of Architecture, University of Liverpool, Liverpool L69 7ZN, United Kingdom, carl.hopkins@liverpool.ac.uk.
[2] Laboratory for Sound Measurement, University of Applied Sciences Rosenheim, Hochschulstraße 1, 83024 Rosenheim, Germany, fabian.schoepfer@fh-rosenheim.de.

Summary

This paper develops and assesses protocols for the measurement of transmission functions in lightweight buildings. A transmission function is defined that relates the spatial-average sound pressure level in a room to the structure-borne sound power injected into a wall or floor. The intention is to facilitate the prediction of structure-borne sound transmission from machinery to receiving rooms. Errors in the measurement of the power input can be reduced by using a pair of accelerometers on either side of the excitation point rather than a single accelerometer on one side. Laboratory measurements on a timber-frame wall indicate that steady-state excitation using an electrodynamic shaker and transient excitation with a force hammer can be considered as equivalent. Measured transmission functions from a laboratory test construction below 500 Hz are found not to be significantly affected by the choice of excitation position being directly above a stud or in a bay. Laboratory and field results on different timber-frame walls indicate that with transient excitation using a force hammer, the transmission function is measurable in vertically-, horizontally- and diagonally-adjacent receiving rooms over the frequency range from 20 to 1 kHz. The approach has been applied in field measurements which indicate that there is potential to create databases of average transmission functions as a simplified prediction tool for sound pressure levels from service equipment in buildings.

PACS no. 43.40.Kd 43.50.Jh 43.55.Rg

1 Introduction

Machinery in buildings acts as a structure-borne sound source which injects vibrational power into the structure. This vibration can propagate across one or more junctions into other rooms where it is re-radiated by the walls and floors. The radiated sound (and sometimes vibration) potentially causes annoyance to the occupants in rooms that are adjacent or distant from the source room which contains the machinery. Hence at the design stage of a new building it is often necessary to be able to estimate the average sound pressure level in a specific receiving room to ensure that the building regulations are satisfied. Two stages are involved to make this estimation. The first stage requires laboratory measurements on a machine from which the structure-borne sound power that is injected into the structure can be determined. The second stage could either use a predictive or an empirical approach to determine the sound pressure level in a specific room. A predictive approach requires a model to calculate structure-borne sound transmission and sound radiation into any room. An empirical approach could be based on measurements that relate the injected structure-borne sound power to the sound power radiated into a room. This would develop the concept of a measured transmission function which can be defined as the ratio of the spatial-average mean-square sound pressure in a receiving room (normalized to the reverberation time) to the injected structure-borne sound power on a wall or floor. The transmission function was introduced in an informative annex of EN 15657–1 [1] to allow a piece of machinery to be fictively connected to a reference configuration of heavyweight walls and floors. For a source room with different powers injected into a wall and a floor and a diagonally-adjacent receiving room the standard illustrates the principle of how transmission functions can be combined to calculate the resultant sound pressure level in the receiving room. In this paper, the aim is to develop a measurement procedure for transmission functions with particular application to lightweight buildings.

The first stage is to characterise the structure-borne sound power that is injected into the structure. Rigorous characterisation of structure-borne sound power is often experimentally demanding (e.g. see [2, 3]). However, for machinery installed in heavyweight buildings, a practical engineering solution to quantify the power input in one-third octave bands or octave bands is to use an isolated reception plate in the laboratory [4, 5, 6]. An isolated plate is necessary because field measurements that treat a wall or floor in a building as a reception plate can introduce significant errors due to energy returning from other coupled walls and floors [7].

The predictive approach to structure-borne sound transmission in the European standard EN 12354–5 [8] is identical to first-order flanking path analysis with Statistical Energy Analysis (SEA) [9]. This standard is primarily intended for heavyweight buildings with receiving rooms that are horizontally-, vertically- or diagonally-adjacent to the source room which contains the machinery. However, higher-order flanking paths are important in most heavyweight buildings, particularly when the receiving room is not adjacent to the source room [10, 11]. EN 12354–5 has an informative annex which attempts to introduce longer paths, but the procedure is unwieldy and it is more efficient to use the matrix approach to SEA rather than use path analysis [9, 10]. The ongoing revision of EN 12354–5 will extend its application to lightweight buildings (i.e. timber or light steel frame) [12]. For heavyweight buildings, the vibration reduction indices used to describe junction transmission can be predicted [13, 14, 15, 16] or measured [17]. However, for lightweight buildings the walls or floors are highly-damped with non-diffuse vibration fields and the junction details are sufficiently complicated such that measurements of the vibration level difference are typically required for inclusion in the model [18]. Building machinery tends to inject high levels of structure-borne sound power in the low-frequency range (e.g. [19, 20, 21]) for which there is the issue of whether the average values predicted by SEA or SEA-based prediction models are adequate. For the above reasons, an empirical approach has the potential to simplify calculations and indicate a range of low-frequency responses when an average transmission function can be identified for specific types of building situations.

Empirical approaches could potentially use a transfer function involving sound pressure or sound power relative to the applied force. Steenhoek and Ten Wolde [22] discussed mechanical-acoustical transfer functions with regards to the advantages of reciprocal measurements. The focus was on transfer functions such as force or velocity at one point on a structure to sound pressure at a specific point in a room which was proposed as a potential transfer function for machinery in buildings. However, this is not practical for most building acoustics applications which usually consider spatial-average sound pressure levels rather than levels at specific points in a room. Further work by Ten Wolde *et al.* [23] developed the concept with further experimental examples; however, these were primarily oriented towards the identification of excitation in each of the six degrees-of-freedom which would be overly complex for the majority of building acoustics applications.

From Cremer *et al.* [24] a reciprocal relationship exists between radiation and response by interchanging excitation and observation points. Using this relationship, Buhlert and Feldmann [25] defined structure-borne sound sensitivity as the ratio of sound power radiated into the receiving room to the mean-square force applied by a machine to the structure, multiplied by a normalisation term. By using the reciprocity relationship and assuming diffuse sound fields, this normalisation allowed the structure-borne sound sensitivity to be determined from measurement of the mean-square pressure at a point in a room and mean-square velocity at the excitation point. As noted by Cremer *et al.* this approach potentially allows the identification of locations to fix machinery that lead to low sound pressure levels in any room. However, most machines have multiple connection points so this might only apply to relatively compact machines. By assuming that the mobility of the receiving structure is much lower than the mobility of the machine, Vercammen and Heringa [26] re-defined structure-borne sound sensitivity as the ratio of sound power radiated into the receiving room to the mean-square force (i.e. without the normalisation term used by Buhlert and Feldmann). They used the reception plate method to give the structure-borne sound power from which the mean-square force was calculated (a similar approach was used by Gerretsen [27]). Arnold and Kornadt [28] considered a transfer function of pressure over the input force as an alternative to the predictive approach of EN 12354–5 for lightweight buildings. This transfer function was measured between horizontally-adjacent rooms with eleven different lightweight separating walls. The transfer functions in decibels were arithmetically averaged to get a spatial-average value, but the variation was between 20 dB and 40 dB. This variation was reduced to between 10 dB and 30 dB by normalizing the transfer function to the driving-point impedance of the excited wall and the reverberation time of the receiving room. An additional step was to normalize to the airborne sound insulation of the wall; whilst this might be a justifiable approximation for horizontally- or vertically-adjacent rooms where the separating wall or floor is excited it would not apply to the general situation. The general conclusion is that transfer functions are a useful tool in the identification of complex forms of excitation over many degrees-of-freedom and for noise control where there is a specific excitation point and a specific receiver point. However, they are less well-suited to the determination of spatial-average sound pressure levels in rooms with uncertain or undefined excitation positions for the machinery.

An empirical approach using transmission functions quantifies the combination of all the transmission paths from the power injected at one or more source positions on an element to a spatial average sound pressure level in a receiving room. For horizontally- or vertically-adjacent rooms the transmission function corresponds to the combination of the direct transmission path and all the flanking paths, but for diagonally-adjacent and more distant rooms it corresponds to the combination of all flanking paths. With the latter, transmission functions could include flanking paths which involve not only bending wave transmission but also in-plane wave transmission. An advantage of the transmission function over transfer functions using mean-square forces is that it is a power-based descriptor which is described by the ratio of sound power to structure-borne sound power. For this reason it is aligned with other approaches commonly used in building acoustics such as prediction models using SEA or SEA-based methods, as well as descriptors such as transmission coefficients for airborne sound insulation.

Machinery can also radiate significant airborne sound although this only tends to be significant in receiving rooms that are horizontally-, or vertically-adjacent to the source room which contains the machinery. This can be incorporated in predictive approaches such as EN 12354–5 for adjacent rooms and in SEA for more distant rooms. Hence it can also be calculated and used alongside the transmission function approach.

In this paper, a methodology is proposed for transmission function measurements by considering the feasibility and implications of using steady-state and transient excitation on lightweight building structures. As building machinery tends to have significant low-frequency structure-borne sound power, this proposal incorporates the low-frequency procedure [29] used for field measurements of sound insulation [30, 31] and in ISO 16032 [32] used for the assessment of service equipment installations in existing buildings. Experimental work on a timber-frame junction in the laboratory is used to investigate the influence of excitation position on the measured transmission function. Laboratory and field measurements using the measurement protocol are used to indicate the range of transmission functions that are likely to occur in practice.

2 Methodology

2.1 General principle

A linear and time-invariant system from source to receiver is assumed. This is appropriate as the levels of vibration generated by machinery in non-industrial buildings are unlikely to induce non-linear response. A wall or floor is mechanically excited and the narrow-band injected power, $W_{\mathrm{NB},k}$, is calculated from the cross-spectrum of the force and velocity at an excitation position, k, as given by

$$W_{\mathrm{NB},k} = 0.5\,\mathrm{Re}\,\{F\,v^*\} \tag{1}$$

where F is the peak force (N) and v^* is the complex conjugate peak velocity (m/s).

The narrow-band injected power level is converted into one-third octave bands to give $L_{\mathrm{W},k}$ at excitation point k which is calculated according to

$$L_{\mathrm{W},k} = 10\lg\left(\frac{\sum_{j=1}^{J} W_{\mathrm{NB},k,j}}{W_0}\right) \tag{2}$$

where $W_{\mathrm{NB},k,j}$ is the injected power for narrow-band j at excitation position k, W_0 is the reference structure-borne sound power of 1E-12 W, and J is the number of narrow bands that form the one-third octave band.

The narrow-band autospectrum for the sound pressure level at microphone position i is converted into one-third octave bands using

$$p_{i,k}^2 = \sum_{j=1}^{J} p_{\mathrm{NB},i,j,k}^2 \tag{3}$$

where $p_{\mathrm{NB},i,j,k}$ is the root mean square pressure for narrow band j at microphone position i with excitation position k. For each microphone position i the one-third octave band sound pressure levels are corrected for background noise.

The spatial-average sound pressure level, $L_{\mathrm{av},k}$ is determined by

$$L_{\mathrm{av},k} = 10\lg\left(\frac{\sum_{i=1}^{M} p_{i,k,\mathrm{corr}}^2}{M\,p_0^2}\right) \tag{4}$$

where $p_{i,k,\mathrm{corr}}^2$ is the one-third octave band mean-square pressure at position i with excitation position k corrected for background noise, M is the number of microphone positions and p_0 is the reference sound pressure of 2E-5 Pa.

If necessary a correction for possible airborne flanking transmission should be applied to the spatial-average sound pressure level, $L_{\mathrm{av},k}$.

The transmission function, $D_{\mathrm{TF},k}$, for an excitation point, k, is defined by

$$D_{\mathrm{TF},k} = L_{\mathrm{av},k} - L_{\mathrm{W},k} \tag{5}$$

The spatial-average transmission function, $D_{\mathrm{TF,av}}$, from K excitation positions is given by

$$D_{\mathrm{TF,av}} = 10\lg\left(\frac{\sum_{k=1}^{K} 10^{0.1 D_{\mathrm{TF},k}}}{K}\right) \tag{6}$$

The standardized spatial-average transmission function, $D_{\mathrm{TF,av,n}T}$, is then given by

$$D_{\mathrm{TF,av,n}T} = D_{\mathrm{TF,av}} - 10\lg\left(\frac{T}{T_0}\right) \qquad (7)$$

where T is the reverberation time in the receiving room and T_0 is the reference reverberation time of 0.5 s. Alternatively, a normalized spatial-average transmission function can be defined using absorption area rather than reverberation time.

Note that there is no normalisation to the reverberation time of the source room in which the excitation is applied. The reason is that in the majority of situations the sound transmitted via an airborne path involving the sound field in the source room will be negligible compared to the structure-borne paths.

2.1.1 Low-frequency measurements

Following the approach in international standards for field sound insulation measurements [30], a low-frequency procedure can be introduced for measurements in the 50, 63 and 80 Hz one-third octave bands where the receiving room has a volume smaller than 25 m^3. However, structure-borne sound from machinery is potentially problematic below 50 Hz; hence measurements to cover the audio low-frequency range in the 20, 25, 31.5, 40, 50, 63 and 80 Hz one-third octave bands can be used on the basis that the low-frequency procedure has been validated down to the 20 or 25 Hz one-third octave bands in previous work in room volumes ranging from 18 to 245 m^3 [29, 33].

The low-frequency procedure in ISO 16283–1 [30] requires additional sound pressure level measurements to be taken using a fixed microphone in the corners of the receiving room at a distance of 0.3 to 0.4 m from each boundary that forms the corner. In ISO 16283–1 a minimum of four corners are measured with two corners at ground level and two corners at ceiling level; however, due to time constraints this paper presents results determined using only two corners, one at ground level and one at ceiling level.

For each excitation position, the highest sound pressure level is determined from the set of measured corners for each of the relevant frequency bands after making any required correction for background noise. For each frequency band, the corner sound pressure level is then calculated using

$$L_{\mathrm{corner},k} = 10\lg\left(\frac{p^2_{\mathrm{corner},k}}{p_0^2}\right) \qquad (8)$$

where $p^2_{\mathrm{corner},k}$ are the highest mean-square sound pressures in one-third octave bands (corrected for background noise where necessary) from corner measurements corresponding to the k^{th} excitation position. Note that for each of the frequency bands, the mean-square sound pressure values needed to calculate $L_{\mathrm{corner},k}$ may be associated with different corners in the room.

The low-frequency energy-average sound pressure level in the relevant frequency bands is calculated by combining $L_{\mathrm{av},k}$ from the default procedure and $L_{\mathrm{corner},k}$ from the low-frequency procedure using

$$L_{\mathrm{av},k,\mathrm{LF}} = 10\lg\left[\frac{10^{0.1L_{\mathrm{av,corner},k}} + (2\cdot 10^{0.1L_{\mathrm{av},k}})}{3}\right] \qquad (9)$$

For the low-frequency bands the transmission function is calculated using Eq. (5) by replacing $L_{\mathrm{av},k}$ with $L_{\mathrm{av},k,\mathrm{LF}}$. If the standardized spatial-average transmission function is then required, it is necessary to measure reverberation times in the low-frequency range. These measurements are problematic if (a) the room volume is small, room modes are sparse and the decays in one-third octave bands are not primarily determined by room modes within the filter pass band, and (b) the reverberation times are sufficiently short that the use of octave bands rather than one-third octave bands becomes essential to avoid measurement errors from the filter and detector in the analyser [29]. The latter is a more common issue in lightweight buildings.

For receiving room volumes smaller than 25 m^3 in one-third octave bands below 100 Hz, the low-frequency procedure used in ISO 16283–1 can be followed where the reverberation time is measured in the 63 Hz octave band to represent the 50, 63 and 80 Hz one-third octave bands [31]. For larger room volumes where room modes occur at frequencies down to the 20 Hz one-third octave band, then the 31.5 Hz octave band could be used to represent the 25, 31.5 and 40 Hz one-third octave bands respectively (and potentially the 20 Hz one-third octave band).

2.2 Steady-state and transient excitation

Steady-state excitation commonly makes use of an electrodynamic shaker; hence a force transducer (or impedance head) needs to be fixed to the wall/floor to measure the injected power at the excitation point. In contrast, transient excitation tends to be applied using a force hammer and therefore no transducers need to be physically connected to the wall/floor. The choice between steady-state and transient excitation is initially determined by whether it is possible to fix a force transducer (or impedance head) to the wall/floor. In lightweight buildings it is often possible to fix a force transducer or impedance head into timber, but this is not usually possible for materials such as plasterboard which are relatively brittle. Hence transient excitation can be useful in many lightweight buildings. However, an important consideration when choosing steady-state or transient excitation is whether it is possible to achieve sufficiently high signal-to-noise ratios for the sound pressure level measurements in the receiving room. If broadband noise signals with shaker excitation require excessively high levels of excitation to give the required signal-to-noise ratio, then it is preferable to use a Maximum Length Sequence (MLS) or a swept-sine signal to obtain the impulse response of a system with increased immunity to noise. The only drawback can be an increase in measurement time.

For field measurements, transient excitation with a force hammer is a practical option because the measurements are relatively quick and require fewer cables. This is particularly useful in the field where there is often intermittent background noise (e.g. road traffic, construction site noise). However, with transients from a metal-tipped force hammer the upper frequency limit tends to be around the 1 kHz one-third octave band, whereas it is feasible to measure to higher frequencies when using steady-state excitation from a shaker. There is also a potential limitation due to non-linearity because the excitation also has to be sufficiently high to achieve a suitable signal-to-noise ratio at the microphones in the receiving room. This is more likely to be an issue with lightweight (rather than heavyweight) buildings at high frequencies where structure-borne sound can be highly-attenuated due to the use of isolated double-leaf constructions and relatively high internal losses. However, structure-borne sound transmission from machinery to distant rooms in a building only tends to be problematic below 1 kHz so this upper frequency limit is not expected to be problematic in many situations. Note that with transient excitation, the measurer stands on the floor; hence for lightweight floors that form a junction with other lightweight walls that are likely to form the dominant transmission path it needs to be checked that the static load of the measurer and/or equipment on the floor does not affect vibration transmission.

This paper uses experimental studies in the laboratory and the field to compare and assess steady-state and transient excitation in order to identify their advantages and disadvantages with lightweight constructions.

2.3 Test constructions and experimental procedures in the laboratory

2.3.1 Laboratory situation: Lightweight construction

A T-junction comprising two timber-frame single walls and a timber joist floor was installed in the transmission suite at the Rosenheim University of Applied Sciences. This junction forms a receiving room downstairs which has a volume of $\approx 50\,\mathrm{m}^3$ to be able to measure transmission functions for horizontal and diagonal transmission as indicated in Figure 1.

The framework for the walls is constructed from vertical timber studs (without noggins), a timber base plate and a timber top plate each with cross-sectional dimensions of 9 x 6 cm. For the floor the timber joists had cross-sectional dimensions of 24 x 6 cm. Each side of the wall and the upper surface of the floor had a single layer of 19 mm chipboard screwed to the timber studs/joists. The cavities were empty (i.e. without sound absorptive material). The spacing for the wall studs and floor joists was 62.5 cm.

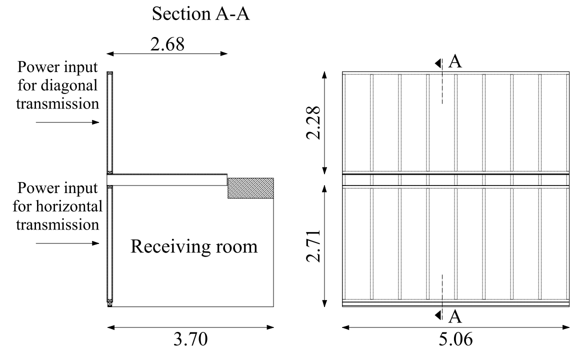

Figure 1: Laboratory test construction: Sketch of cross-section through T-junction (dimensions in metres).

The junction between the walls and the floor is rigidly connected. Every floor joist was screwed to the frame of the lower wall before the framework of the upper wall was mounted and fixed with screws to the floor joists.

The lower wall of the T-junction and the joists of the floor were supported on resilient mounts to decouple them from the rest of the laboratory building; this resulted in a junction with a mass-spring resonance frequency of ≈ 20 Hz above which it was isolated from the ground floor. All other boundaries of the T-junction were free (i.e. disconnected from other parts of the structure).

2.3.2 Laboratory measurements: Comparison of steady-state and transient excitation

For diagonal transmission, the excitation point on the wall was on the chipboard directly above a vertical timber stud. For steady-state excitation, a washer was glued to the surface of the chipboard in order to mount the force transducer. For transient excitation, a force hammer with a metal hammer tip was used to impact the chipboard.

For horizontal transmission, two different excitation points were used, one directly above a vertical timber stud and another in the bay between two adjacent vertical timber studs. For steady-state excitation on a stud, a washer was glued to the surface of the chipboard and screwed into the timber stud in order to mount the force transducer and only glued to the surface of the chipboard for excitation in a bay.

Transient excitation was applied using an impact hammer (Endevco, Type 2302-10) with rubber and metal tips and steady-state excitation was applied using an electrodynamic shaker (Bruel & Kjær, Type 4810) with an MLS signal (Norsonic RTA 840). A force transducer (MMF, Type KF24) was used in-line with the shaker.

To determine the power input for both transient and steady-state excitation, two accelerometers (MMF, Type KS95B100) were mounted on either side of the excitation point to estimate the response at the driving point from averaged signal. The power input was calculated from (1) the pair of accelerometers, A and B, to give a time-average signal from $(A+B)/2$ and (2) a single accelerometer A.

Sound pressure in the receiving room was measured using three microphones; one Norsonic Type 1220 (with a Norsonic pre-amplifier Type 1201) and two low-noise microphones (G.R.A.S. half-inch low-noise microphone Type 40HL). The same microphone positions were used for transient and steady-state excitation. The transmission function between power input and mean sound pressure level was determined as described in section 2.1.

For diagonal transmission and transient excitation, the same protocol was used as for horizontal transmission. For steady-state excitation, time limitations meant that only measurements with white noise were possible; hence MLS results were not available. The sound pressure was measured using the same multichannel FFT analyser as for the force and the accelerations at the excitation point.

The average sound pressure level was corrected for airborne flanking transmission; however, this was negligible in most cases because the structure-borne path was usually dominant.

2.3.3 Laboratory measurements: Limitations related to measurement of the power input with a pair of accelerometers

To determine the power input with steady-state excitation the applied force and the response at the driving point can either be determined using an impedance head or a force transducer in combination with one or more accelerometers. For the latter the only option is to put the accelerometer(s) adjacent to the driving point because there is no access inside the wall or floor to position an accelerometer directly behind the excitation point. With transient excitation from a force hammer the only option is to put the accelerometer(s) adjacent to the excitation point. As a rule-of-thumb the aim is to position the accelerometer(s) at a distance, d, from the excitation point such that $k_\mathrm{B}\, d \ll 1$ [9] where k_B is the bending wavenumber.

To assess the errors involved in using accelerometers adjacent to the excitation point, a free-hanging panel was used so that there was access to both sides. This

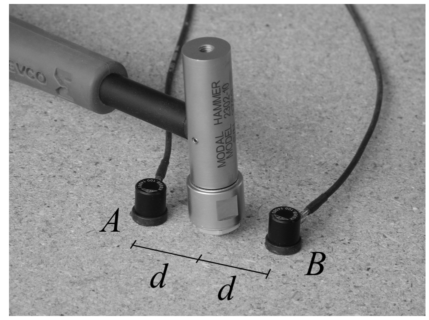

Figure 2: Force hammer excitation with accelerometers A and B with a separation distance, d.

panel was 19 mm chipboard (2.05 x 0.92 m) as was used in the laboratory test construction. The power input was measured with transient excitation from a force hammer (Endevco, Type 2302-10) and three accelerometers. Two accelerometers, A and B, (MMF, Type KS95B100) were positioned on the source side of the chipboard equidistant from the excitation point at distances between 1 and 10 cm using 1 cm steps that were measured from the centre of the force hammer tip to the centre of each accelerometer (see Figure 2). In addition, accelerometer C (MMF, Type KS95B100) was positioned directly opposite the excitation point on the reverse side of the chipboard, and this was assumed to give the most accurate estimate of the actual power input. For these accelerometers the diameters were ≈ 11 mm which is a practical minimum diameter which allows the accelerometers to be close to the excitation point and avoid spatial summation of the response over too large an area.

2.3.4 Laboratory measurements: Spatial variation of excitation positions

To investigate the influence of excitation position on the transmission function, measurements were carried out on the laboratory construction. For horizontal and diagonal transmission, the transmission function was measured at a number of excitation points which represented potential fixing points for service equipment. For horizontal transmission with excitation on the lower wall and diagonal transmission with excitation on the upper wall, measurements were carried out to assess the variation between excitation points on bay and stud positions. For diagonal transmission, measurements were also carried out to assess the effect of distance from the T-junction; this was not carried out for horizontal transmission as the direct transmission path across the wall was assumed to be dominant. The excitation positions on the upper wall (diagonal transmission) and lower wall (horizontal transmission) are shown in Figures 3 and 4 respectively.

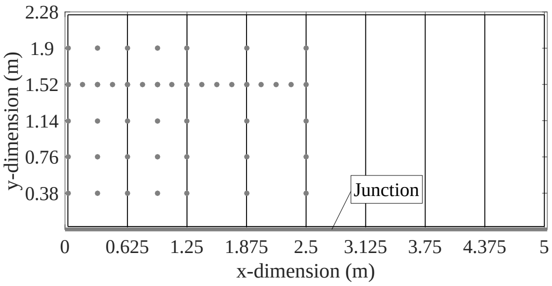

Figure 3: Excitation positions on the upper wall for diagonal transmission (45 excitation positions).

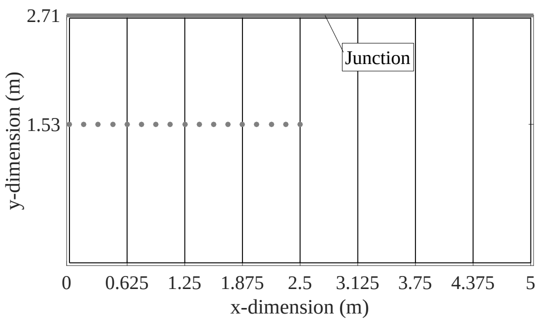

Figure 4: Excitation positions on the lower wall for horizontal transmission (17 excitation positions).

2.4 Test constructions and experimental procedures in the field

2.4.1 Case study

To assess the measurement of transmission functions from a source room (SR) to the adjacent receiving room (RR1) and non-adjacent receiving rooms (RR2, RR3, RR4) in the horizontal direction, field measurements were carried out in an unoccupied timber-frame building with a regular floor plan as shown in Figure 5. The transmission function was determined using transient excitation with a force hammer and steady-state excitation using an electrodynamic shaker with MLS (MLS signal-to-noise ratio was at least 6 dB). In each receiving room the sound pressure was measured at four positions in the central zone of the room and two positions in corners.

All the test rooms were cuboids with a volume of $35.2\,\mathrm{m}^3$ (2.71 x 5.20 x 2.50 m). The timber-frame separating walls were built with two layers of plasterboard (12.5 mm gypsum board and 25 mm gypsum fibre board) on one side, and 25 mm gypsum fibre boards on the other side screwed to laths mounted on resilient channels that were perpendicular to the framework of the wall. These separating walls had a sound reduction index of $\approx 58\,\mathrm{dB}\ R_\mathrm{w}$. Each room had a suspended ceiling as well as a floating screed on the floor.

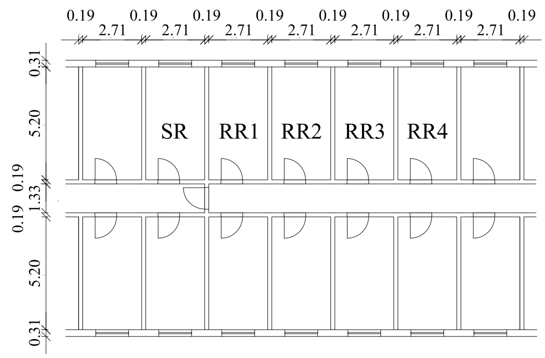

Figure 5: Field test construction: Ground floor plan of the timber-frame building (dimensions in metres).

2.4.2 Comparison of different field constructions

To gain initial insights into the range of transmission functions that exist in different lightweight buildings, field measurements were taken in seven timber-frame buildings (single family houses, guesthouses and apartment buildings) built by two different companies. These measurements were scheduled at the end of the construction process just before transfer to the residents; hence all the main construction work had been completed. Several transmission functions were measured in each building for horizontally, vertically or diagonally adjacent rooms. Only walls were excited because every building had a floating screed on the base floor. In total, 34 transmission functions were measured.

Only transient excitation was carried out with a force hammer using two or three excitation positions. Where possible, one position was chosen in a bay and another above or close to a stud but there was some uncertainty as to the exact positions due to the finished surface obscuring the exact positions of the studs. The injected power was determined using two accelerometers with the force hammer described in section 2.3.3 and accelerometer spacing, d, of 2 to 2.5 cm. The average sound pressure level in the receiving room was measured using four positions in the central zone of the room and two corner positions (rather than four corner positions in order to reduce on-site measurement time). The sound pressure levels were corrected for background noise or rejected if the signal level was below the background noise level. In addition, the average sound pressure level was corrected for airborne flanking transmission; however, this was negligible in most cases as the structure-borne path was usually dominant.

The different types of construction were timber-frame single walls with plasterboard on both sides, timber-frame single walls with plasterboard on both sides with additional plasterboard lining (used to con-

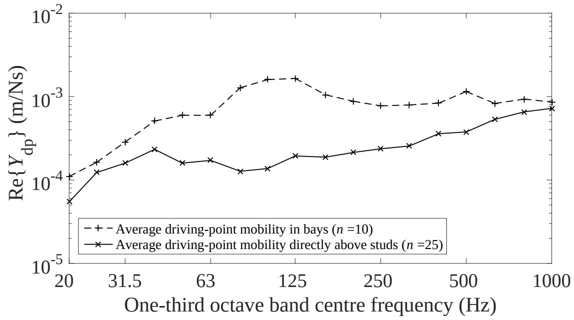

Figure 6: Laboratory measurements. Comparison of the spatial-average driving-point mobility in bays and directly above studs.

tain pipework in bathrooms and kitchens), interior and exterior framed walls, timber-frame double walls with individual frames (party wall), and masonry or concrete walls in basements where the transmission was measured to timber-frame single walls (plasterboard on both sides) on the ground floor.

3 Results

3.1 Laboratory measurements: Comparison of steady-state and transient excitation

Figure 6 shows that there are significant differences in the measured driving-point mobility in bays compared to directly above the studs. This has also been shown to occur with other lightweight constructions, e.g. see [34]. For this reason, the measurements were taken with excitation in bays and directly above the studs.

A comparison of transmission functions determined with steady-state and transient excitation are shown in Figure 7 for the following three cases:

(1) Horizontal transmission with excitation directly above a stud. For steady-state excitation, a washer was glued to the surface of the chipboard and screwed into the stud in order to mount the force transducer. For transient excitation with a force hammer, a rubber tip was used in the 20, 25 and 31.5 Hz one-third octave bands, and a metal tip at and above the 40 Hz one-third octave band (Figure 7(a)).

(2) Horizontal transmission with excitation in a bay. For steady-state excitation, a washer was glued to the surface of the chipboard to mount the force transducer. For transient excitation with a force hammer, a rubber tip was used in the 20, 25 and 31.5 Hz one-third octave bands and a metal tip at and above the 40 Hz one-third octave band (Figure 7(b)).

(3) Diagonal transmission with excitation on the chipboard directly above a stud. For steady-state excitation, a washer was glued to the surface of the chipboard to mount the force transducer (NB The signal-to-noise ratio when using steady-state excitation was

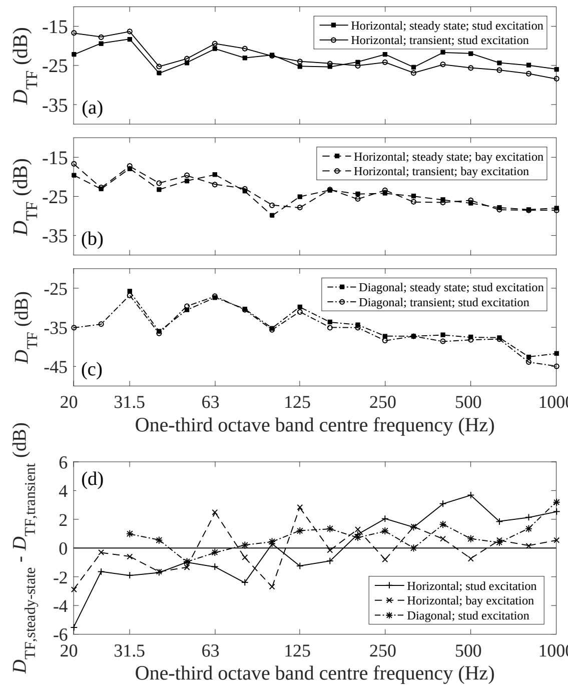

Figure 7: Laboratory measurements. Comparison of transmission function for steady-state and transient excitation:
(a) horizontal transmission with excitation on a stud,
(b) horizontal transmission with excitation in a bay,
(c) diagonal transmission with excitation on a stud,
(d) difference between transmission functions determined using transient and steady-state excitation.

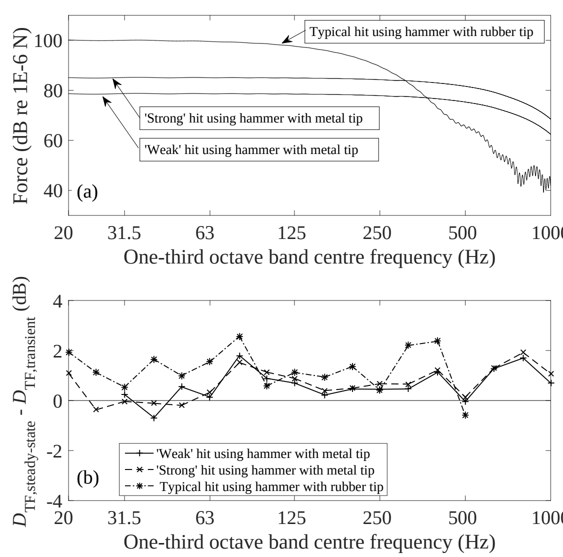

Figure 8: Laboratory measurements. Investigation into the effect of different strength of transient excitation: (a) different force levels of the transient excitation with the force hammer, (b) difference between transmission functions determined using transient and steady-state excitation.

too low in the 20 and 25 Hz one-third octave bands to yield data). For transient excitation with a force hammer, a metal tip was used (Figure 7(c)).

For one-third octave bands from 31.5 to 1 k Hz the differences between steady-state and transient excitation in all three cases are typically ±2 dB although it is ±5.5 dB at 20 Hz (Figure 7(d)). For horizontal transmission with stud excitation where the shaker was attached directly to the stud using screws through the chipboard, the difference between steady-state and transient excitation above 250 Hz is ≈ 2.5 dB whereas it is only ≈ 0.5 dB with bay excitation. The differences could partly be due to the different mounting conditions for which the glued and screwed washer used with steady-state excitation could apply a force directly to the stud which would not occur with transient excitation; however, there is no systematic difference across the frequency range. As building machinery often has significant structure-borne sound power input at frequencies up to 250 Hz, the fact that both methods are in reasonable agreement leads to the conclusion that both methods can be used for field measurements.

To investigate differences between transient and steady-state excitation in the laboratory, different force levels were applied with a force hammer as indicated in Figure 8 (a). With the force hammer, a metal tip was used to give a 'weak' and a 'strong' hit (although with the 'weak' hit the signal-to-noise ratio was only > 6 dB at and below the 25 Hz one-third octave band and therefore these bands were rejected). A rubber tip was also used that gave signal-to-noise ratios > 10 dB up to 500 Hz. The comparison of transient with steady-state excitation is shown in Figure 8 (b) for horizontal transmission. To exclude variations due to microphone positioning, only one fixed microphone in the receiving room was used instead of several positions. The results indicate that transient excitation with metal or rubber tip gives ≈ 1 dB lower values (on average) than steady-state excitation up to 1 k Hz. However, this occurs with both the 'weak' and 'strong' hits so there is no conclusive evidence of non-linearity with high levels of transient excitation. For most engineering applications it is therefore reasonable to opt for the most convenient form of excitation which will usually be transient excitation with a force hammer.

3.2 Laboratory measurements: Limitations related to measurement of the power input with transient excitation

This section assesses the limitations related to measurement of power input (as described in Section 2.3.3) when accelerometers can only be positioned adjacent to, rather than directly behind, the excitation position. The measured power input from a single accelerometer and a pair of accelerometers were normalized to the power input calculated from the accelerometer directly opposite the excitation point on the reverse side of the chipboard as the latter was assumed to give the most accurate estimate. The normalized power inputs are shown on Figure 9 in terms of d/λ_B, as this is a more practical descriptor than the bending wavenumber, k_B. This indicates that if a pair of accelerometers is used rather than a single accelerometer, then the errors are significantly reduced and are a smoother function of d/λ_B. For a pair of accelerometers, the error is ≤ 1 dB when $d/\lambda_\mathrm{B} \leq 1/10$ (and ≤ 3 dB when $d/\lambda_\mathrm{B} \leq 1/6$). To put this in context for a 19 mm chipboard plate, $d/\lambda_\mathrm{B} = 1/10$ corresponds to a frequency of ≈ 1.7 k Hz when $d = 2$ cm. Although transient excitation was used, the benefit of using a pair of accelerometers also applies when excitation is applied using an electrodynamic shaker.

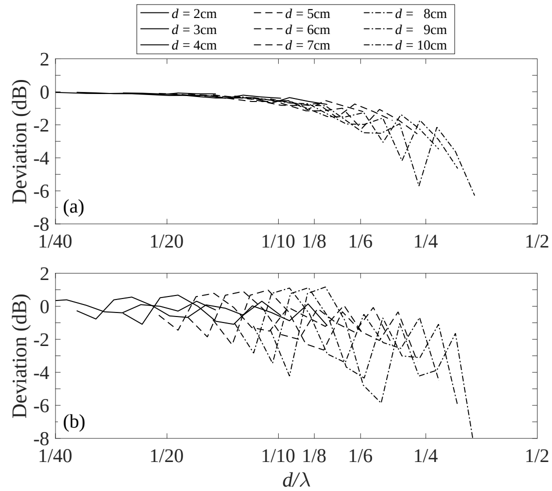

Figure 9: Power input for (a) a pair of accelerometers and (b) a single accelerometer on the same side as the excitation point normalized to the power input using the accelerometer directly opposite the excitation point on the reverse side of the chipboard.

3.3 Laboratory measurements: Spatial variation of excitation positions on lightweight structures

The effect of different excitation positions on the transmission function is investigated by considering the distance to the nearest stud. In addition, for diagonal transmission the distance to the junction was also considered. Five different distances for positions in the middle of two bays and above five studs were chosen. For horizontal and diagonal transmission, measurement positions were used on a line perpendicular to the studs. Three groups of excitation positions were considered: (1) five positions above a stud, (2) four positions in the middle of each bay and (3) eight positions at a distance of 15 cm from the centre line

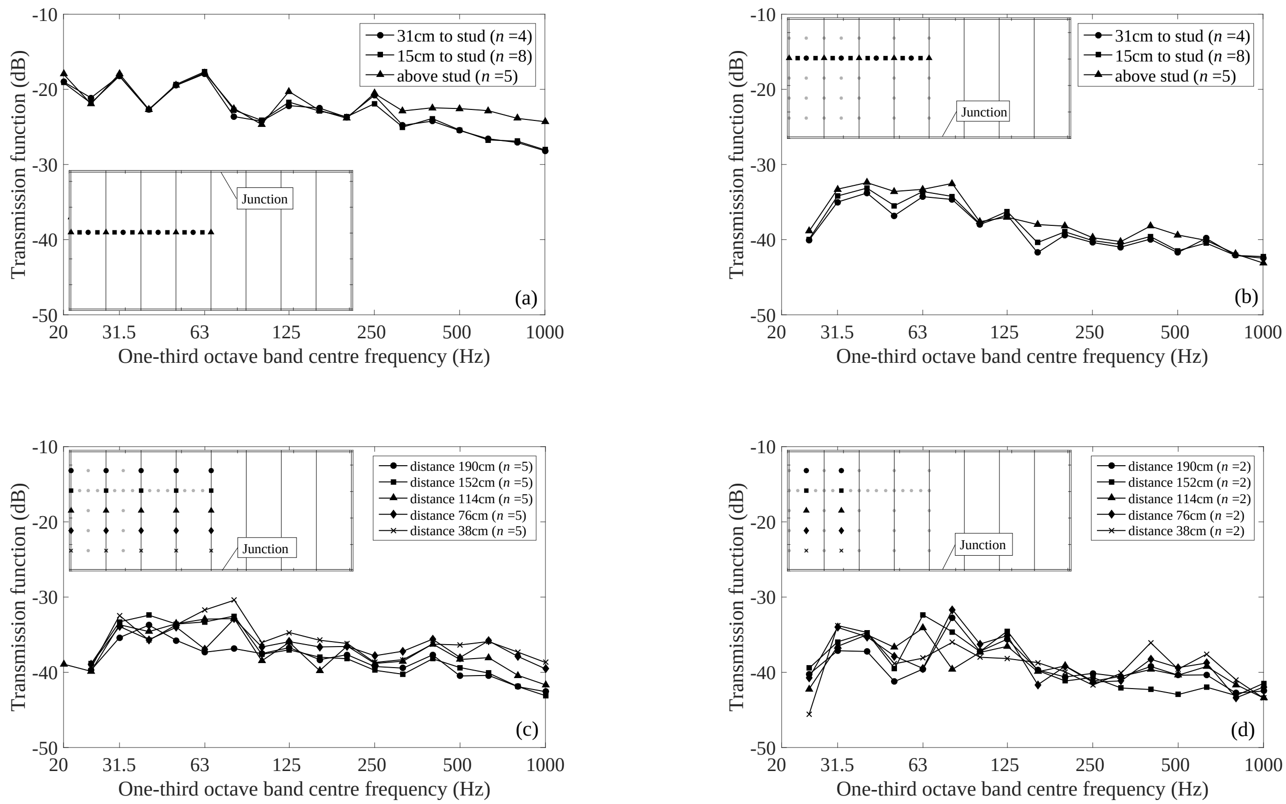

Figure 10: Laboratory measurements. Average transmission functions.
(a) Horizontal transmission measured above the stud and at different distances from the stud in the bay.
(b) Diagonal transmission measured above the stud and at different distances from the stud in the bay.
(c) Diagonal transmission measured above the stud at different distances from the junction.
(d) Diagonal transmission measured in the bay at different distances from the junction.

---

of the studs.

Figure 10 shows the average transmission functions. For each curve in Figures 10 (a), (b) and (c) the 95% confidence interval was ≈ 3 dB (Student t distribution), and for Figure 10 (d) the range for each pair of points was ≈ 3 dB. Hence in Figure 10 (a) the only region in which the confidence intervals don't overlap is between 500 and 1 k Hz. On (b), (c) and (d) the degree of uncertainty in these average values means that there is no strong dependence of the transmission function on excitation position.

Figures 10 (a) and 10 (b) show the average transmission function for each of these three groups for horizontal and diagonal transmission respectively. For horizontal transmission the results only differ by ± 3 dB below 315 Hz. Above 315 Hz the positions above the studs have the highest value which indicates that transmission is strongest for this type of excitation position; this is likely to be due to more efficient transfer via the structure-borne path across the stud compared to the path involving the sound field in the cavity. For diagonal transmission the results only differ by ± 4 dB over the frequency range from 20 to 1 k Hz. In comparison to horizontal transmission it seems that the influence of varying the excitation position is less important with increasing complexity of the transmission path.

For diagonal transmission, positions with five different distances to the junction were measured directly above the studs or in the middle of a bay as shown in Figures 10 (c) and 10 (d). In each case the results vary by ± 4 dB (on average) below 500 Hz. For stud excitation above 500 Hz there are indications that the excitation positions closest to the junction give the highest transmission functions. For bay excitation, the effect of distance to the junction is negligible in this case; this might be due to the empty cavities and it is hypothesised that this might be different if the cavities were filled with absorbent material.

It is concluded that below 500 Hz the measured transmission function is not significantly affected by the choice of excitation position (i.e. directly above a stud or in a bay).

Figure 11 shows the average transmission function with error bars indicating the 95% confidence limits (Student t distribution) for 17 excitation positions for horizontal transmission and for the 45 excitation positions for diagonal transmission. The 95% confidence limits are approximately ± 2 dB for horizontal, and approximately ± 1 dB for diagonal transmission across the frequency range from 20 to 1 k Hz. For diagonal transmission the signal-to-noise ratio was not sufficient to measure the 20 Hz one-third octave band. It is notable that the curves are relatively uniform, and tend to decrease with increasing frequency. As they are relatively featureless curves it might be feasible to establish average values for a broad frequency range. This is considered further with field measurements in the next section.

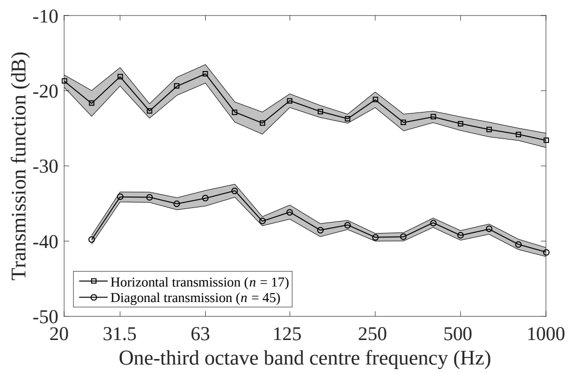

Figure 11: Laboratory measurements. Transmission functions for horizontal and diagonal transmission. Results are shown as an average value from positions above studs and between studs with shaded area indicating the 95% confidence limits (Student t distribution).

3.4 Field measurements

Figure 12 shows the average signal-to-noise ratio for receiving rooms RR1, RR2 and RR3 for metal and rubber tips on the force hammer where values below 6 dB were rejected. In receiving room RR1, the signal-to-noise ratio is > 10 dB up to 1 k Hz for both the metal and the rubber tips. However, the rubber tip can provide a higher signal-to-noise ratio than the metal tip below 250 Hz. For the non-adjacent rooms (RR2 and RR3) it was not possible to measure in all bands between 20 and 1 k Hz with signal-to-noise ratios > 10 dB and in this particular field measurement the background noise was particularly high at 125 Hz which prevented it being possible to measure in that band.

The findings indicate that transient excitation can be used for lightweight timber party walls to measure the transmission function between adjacent rooms. For measurements between 20 and 1 k Hz it is reasonable to use a metal tip. Measurements with a rubber tip can be used to increase the signal-to-noise ratio by a few decibels below 100 Hz. Depending on the frequency range of interest, a metal tip, a rubber tip or a combination of both can be used. For non-adjacent rooms, transient excitation is only likely to be feasible for the whole frequency range from 20 to 1 k Hz in buildings with very low background noise.

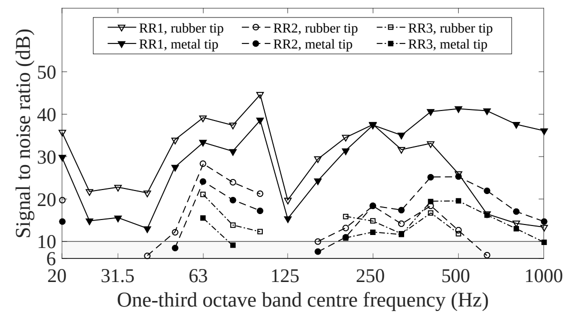

Figure 12: Field measurements. Signal-to-noise ratio in receiving rooms RR1, RR2, and RR3 for transient excitation. Grey shading indicates signal-to-noise ratios between 6 and 10 dB.

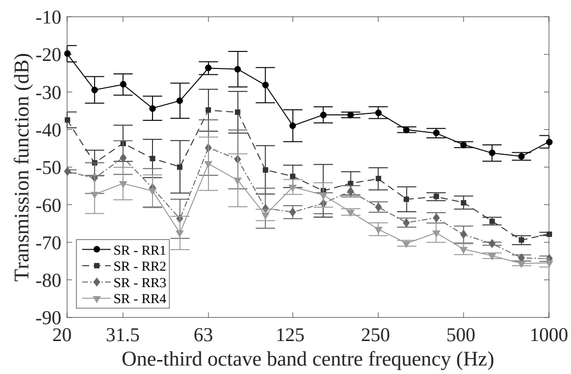

Figure 13: Field measurements. Transmission function to receiving rooms measured using an electrodynamic shaker and MLS at one excitation position. Results are shown as an average value with error bars indicating the 95% confidence limits (Student t distribution) where the variation is due to individual microphone positions.

As it was not feasible to use transient excitation to measure transmission functions to non-adjacent rooms in this particular case, measurements were taken using MLS excitation. Figure 13 shows the transmission functions determined from the source room (SR) to four receiving rooms (RR1, RR2, RR3, RR4). The transmission function to the adjacent receiving room (RR1) is at least 11 dB higher than to the non-adjacent receiving rooms (RR2, RR3, RR4). The transmission functions for the non-adjacent receiving rooms (RR2, RR3, RR4) tend to be within 10 dB of each other which indicates the importance of flanking transmission.

To try and identify an average transmission function for different constructions, transmission functions for the different field constructions were grouped in terms of the direction of transmission (i.e. horizontal, vertical or diagonal) and the type of construction. For the latter, the constructions were divided into four groups: (1) single framework without additional lining (common interior walls), (2) single framework with additional lining (common interior walls in bathrooms), (3) interior and exterior framed walls and (4) separated framework (party walls). With the available data is was possible to form five groups from the combination of these grouping criteria with at least two measured transfer functions for each combination. A sixth group is formed by transmission functions measured from the basement to a ground floor room. Since the basement is usually the place where household appliances are installed, this is an important path. On this path there is usually a masonry or concrete wall in the basement separated with a concrete floor to the timber-frame construction above. The grouped transmission functions are shown in Figure 14 which are in terms of $D_{\mathrm{TF,av}}$ (calculated according to equation 6) for the 20 to 40 Hz one-third octave bands and $D_{\mathrm{TF,av,n}T}$ (calculated according to equation 7) for one-third octave bands at and above 50 Hz. Below 100 Hz the low-frequency procedure was applied as described in section 2.1.1.

For horizontal transmission across single timber-frame constructions (i.e. typical internal walls within single-family houses) the spread of results is ≈ 20 dB over the frequency range from 20 to 1 k Hz – see Figure 14(a). The lowest transmission function was an outlier in this group which could be attributed to additional cross battens that were screwed to the framework on one side that meant it was not suitable for the chosen grouping. Excluding this outlier means that the main group has a variation of ≈ 15 dB. As with the laboratory results (refer back to Figure 11) the spectral shape is relatively uniform, and decreases with increasing frequency. Only three measurements were available for horizontal transmission across typical internal walls with an additional lining and whilst two of the three results are similar to those without an additional lining there is one outlier that has a significantly lower transmission function due to a decoupled lining – see Figure 14(b).

For diagonal transmission across single timber-frame constructions, three measurements are shown in Figure 14(c) for which the variation is ≈ 10 to 20 dB. In the 20, 25 and 31.5 Hz one-third octave band results are only available for one or two of the datasets due to insufficient signal-to-noise ratios.

For vertical transmission with interior and exterior timber framework walls, the results are shown in Figure 14(d). The results for these four situations show a spread of ≈ 10 to 20 dB.

For horizontal transmission across a timber-frame double wall with individual frames (party wall), the isolation between these frames results in a significant decrease in the transmission function with increasing frequency – see Figure 14(e). However, in one-third octave bands below 50 Hz the transmission function is similar to those for a single timber-frame (Figure 14(a)).

For both vertical and diagonal transmission, the transmission path from a masonry or concrete wall in the basement to a framework construction in the ground floor results in a spread of ≈ 10 dB as shown in Figure 14(f). In one-third octave bands below 63 Hz the signal-to-noise ratio was not sufficient. In general, the transmission function tends to be slightly higher than with diagonal or vertical transmission in timber-frame constructions.

In general, there was a spread of transmission function values up to 20 dB when grouping similar constructions and transmission directions in this study. The transmission function curves do not show prominent features and vary uniformly with frequency; hence it should be feasible to identify average values for different types of constructions. These results are the first step in identifying typical spectral features of the transmission function for lightweight constructions. The general trend for horizontal transmission is that the spectrum is relatively flat, except for double walls where the spectrum tends to rapidly fall-off with increasing frequency. For vertical and diagonal transmission, the spectrum tends to slowly fall-off with increasing frequency. Below 50 Hz there is evidence that all types of construction give a similar transmission function regardless of whether there is horizontal, vertical or diagonal transmission. However, this dataset is relatively small, and future work will need to collect larger datasets in order to give guidance suitable for building regulations. Issues that need consideration include whether it is necessary to restrict the range of room volumes that are used to determine the average response in the low-frequency range, particularly when considering frequencies down to 20 Hz, and whether it is possible to consider timber-frame and light-steel frame structures as a single group when the cavity is empty (i.e. no absorbent material).

4 Conclusions

The prediction of structure-borne sound transmission from machinery in lightweight buildings can be considered by using measured transmission functions that relate the spatial-average sound pressure level in a room to the structure-borne sound power injected into a wall or floor. An advantage with this power-based descriptor is that it is aligned with other approaches commonly used in building acoustics such as prediction models using SEA or SEA-based methods (i.e. EN 12354), as well as descriptors such as transmission coefficients for airborne sound insulation. The transmission function approach does not identify the strength of individual transmission paths but for future work it does allow validation of models which can give these insights.

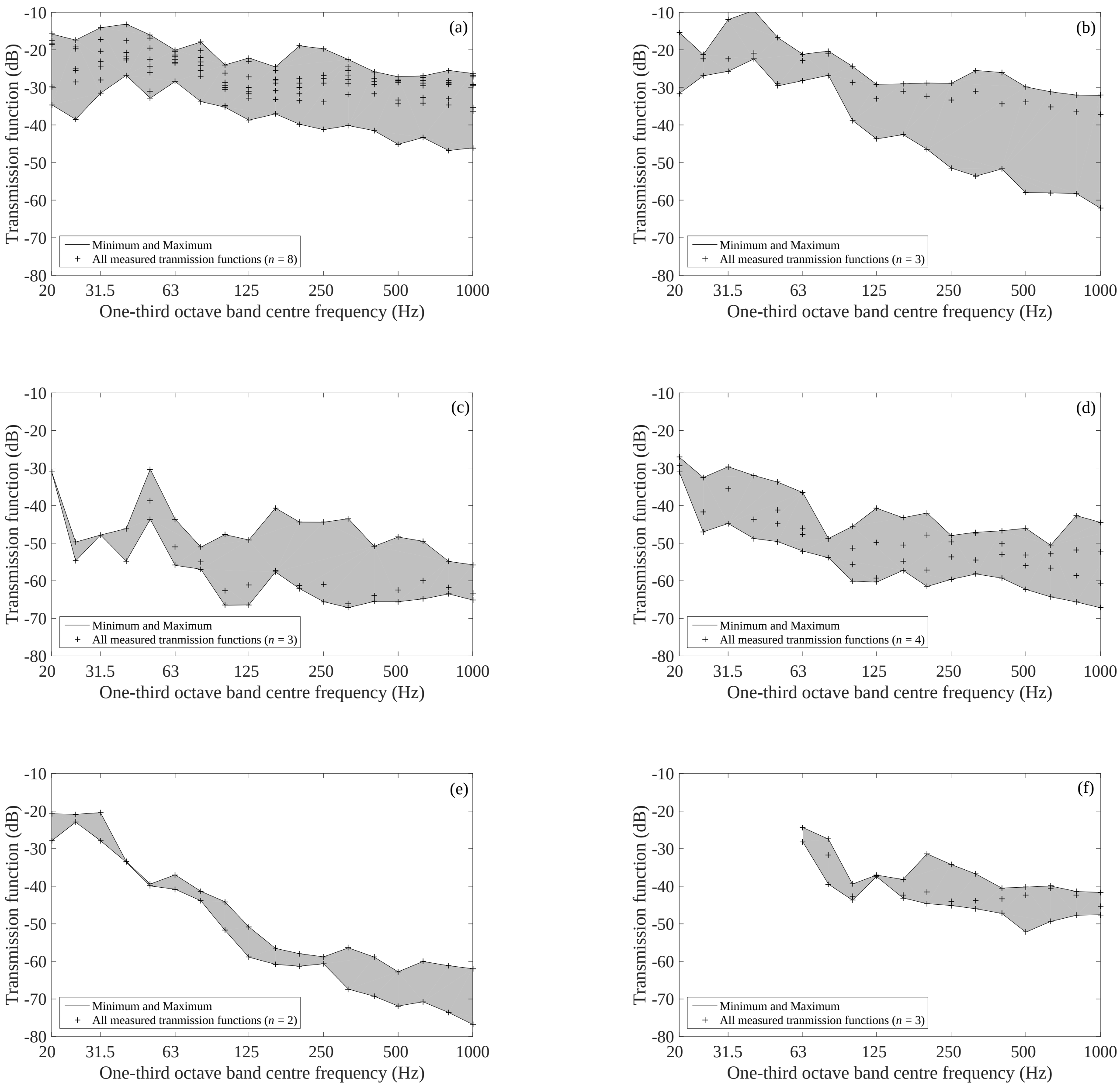

Figure 14: Field measurements. Summary of transmission functions measured with transient excitation in adjacent rooms.
(a) Timber-frame single wall with plasterboard on both sides, horizontal transmission
(b) Timber-frame single wall with plasterboard on both sides, horizontal transmission, with additional plasterboard lining (used to contain pipework in bathrooms and kitchens).
(c) Timber-frame single wall with plasterboard on both sides, diagonal transmission
(d) Interior and exterior timber-frame walls (single and double), vertical transmission
(e) Timber-frame double wall with individual frames (party wall), horizontal transmission
(f) Masonry or concrete wall in basement to timber-frame single wall with plasterboard on both sides on the ground floor, vertical and diagonal transmission

Laboratory measurements of transmission functions on a timber-frame wall show that steady-state excitation using an electrodynamic shaker and transient excitation with a force hammer can be considered as equivalent. It is shown that errors in the measurement of the power input can be reduced by using a pair of accelerometers on either side of the excitation point rather than a single accelerometer on one side. Below 500 Hz the measured transmission function is not significantly affected by the choice of excitation positions being directly above a stud or in a bay.

Laboratory and field results on different types of timber-frame walls indicate that with transient excitation using a force hammer, the transmission function is measurable in vertically-, horizontally- and diagonally-adjacent receiving rooms over the frequency range from 20 to 1 k Hz. For non-adjacent rooms (i.e. distant rooms in a building) it is likely that an electrodynamic shaker will be required using MLS or swept-sine signals.

Field measurements indicate that there is potential to create databases of average transmission functions as a simplified prediction tool. This would allow estimation of noise from the same equipment installed in buildings which are built from different elements with a similar room layout. Future work involving the application of such databases will need to focus on the rules needed to define the grouping of different constructions.

Acknowledgement

This work is part of a research project carried out in cooperation with the Hochschule für Technik Stuttgart and the Acoustics Research Unit at the University of Liverpool. It was funded by the German Federal Ministry of Education and Research within the program FHProfUnt (Grant reference 03FH089PB2). The authors would also like to thank Müller-BBM Vibro Akustik Systeme GmbH for their support with the measurement system and equipment. Many thanks also go to Regnauer Fertighaus GmbH for the support in planning and construction of the laboratory test rig as well as providing buildings for the field measurements.

References

[1] EN 15657-1:2009. Acoustic properties of building elements and of buildings – laboratory measurement of airborne and structure-borne sound from building equipment. Part 1: Simplified cases where the equipment mobilities are much higher than the receiver mobilities, taking whirlpool baths as an example.

[2] J. M. Mondot and B. A. T. Petersson. Characterization of structure–borne sound sources: the source descriptor and the coupling function. *Journal of Sound and Vibration*, 114(3):507–518, 1987.

[3] A. T. Moorhouse, A. S. Elliott, and Evans. T. A. In situ measurement of the blocked force of structure-borne sound sources. *Journal of Sound and Vibration*, 325(4):679–685, 2009.

[4] M. M. Späh and B. M. Gibbs. Reception plate method for characterisation of structure-borne sources in buildings: Assumptions and application. *Applied Acoustics*, 70:361–368, 2009.

[5] B. M. Gibbs, R. D. Cookson, and N. Qi. Vibration activity and mobility of structure-borne sound sources by a seception plate method. *The Journal of the Acoustical Society of America*, 123(6):4199–4209, 2008.

[6] A. R. Mayr and B. M. Gibbs. Single equivalent approximation for multiple contact structure-borne sound sources in buildings. *Acta Acustica united with Acustica*, 98:402–410, 2012.

[7] C. Hopkins and M. Robinson. Using transient and steady-state SEA to assess potential errors in the measurement of structure-borne sound power input from machinery on coupled reception plates. *Applied Acoustics*, 79:35–41, 2014.

[8] EN 12354-5:2009. Building acoustics – estimation of acoustic performance of building from the performance of elements. Part 5: Sound levels due to the service equipment.

[9] C. Hopkins. *Sound Insulation*. Butterworth-Heinemann, 2007.

[10] R. J. M. Craik. *Sound transmission through buildings: Using Statistical Energy Analysis*. Gower, Aldershot, England and Brookfield, Vt., USA, 1996.

[11] R. J. M. Craik. The contribution of long flanking paths to sound transmission in buildings. *Applied Acoustics*, 62:29–46, 2001.

[12] C. Guigou-Carter, M. Villot, and R. Wetta. Prediction method adapted to wood frame lightweight constructions. *Building Acoustics*, 13(3):173–188, 2006.

[13] C. Hopkins. Determination of vibration reduction indices using wave theory for junctions in heavyweight buildings. *Acta Acustica united with Acustica*, 100(6):1056–1066, 2014.

[14] C. Crispin, L. De Geetere, and B. Ingelaere. Extensions of EN 12354 vibration reduction index expressions by means of FEM calculations. In *Proceedings of Internoise 2014, 16-19 November, Melbourne, Australia*, 2014.

[15] J. Poblet-Puig and C. Guigou-Carter. Using spectral finite elements for parametric analysis of the vibration reduction index of heavy junctions oriented to flanking transmissions and EN 12354 prediction method. *Applied Acoustics*, 99:8–23, 2015.

[16] C. Hopkins, C. Crispin, J. Poblet-Puig, and C. Guigou-Carter. Regression curves for vibration transmission across junctions of heavyweight walls and floors based on finite element methods and wave theory. *Applied Acoustics*, 113:7–21, 2016.

[17] ISO 10848-1:2006-08. Acoustics – laboratory measurement of the flanking transmission of airborne and impact sound between adjoining rooms. Part 1: Frame document.

[18] M. Villot and C. Guigou-Carter. Measurement methods adapted to wood frame lightweight constructions. *Building Acoustics*, 13(3):189–198, 2006.

[19] J. M. Scheck, S. Reinhold, P. Eschbach, and H.-M. Fischer. Messung und prognose der luft- und körperschallübertragung von gebäudetechnischen anlagen im massivbau. In *Procedings of DAGA 2016, 14-17 March, Aachen, Germany*, 2016.

[20] A. Vogel, J. Arnold, O. Kornadt, C. Völker, and V. Wittstock. Prediction of sound pressure levels in rooms using EN 12354 and the characteristic structure-borne sound power of structure-borne sound sources. In *Proceedings of Internoise 2016, 21-24 August, Hamburg, Germany*, 2016.

[21] A. R. Mayr and B. M. Gibbs. Approximate method for obtaining source quantities for calculation of structure-borne sound transmission into lightweight buildings. *Applied Acoustics*, 110:81–90, 2016.

[22] H. F. Steenhoek and T. Ten Wolde. The reciprocal mesurement of mechanical-acoustical transfer functions. *Acustica*, 23:301–305, 1970.

[23] T. Ten Wolde, J. W. Verheij, and H. F. Steenhoek. Reciprocity method for the measurement of mechano-acoustical transfer functions. *Journal of Sound and Vibration*, 42(1):49–55, 1975.

[24] L. Cremer, M. Heckl, and E. E. Ungar. *Structure-borne sound: Structural vibrations and sound radiation at audio frequencies.* Springer, Berlin, 2. ed. edition, 1988.

[25] K.-J. von Buhlert and J. Feldmann. Ein meßverfahren zur bestimmung von körperschallanregung und -übertragung. *Acustica*, 42(3):108–113, 1979.

[26] M. L. S. Vercammen and P. H. Heringa. Characterising structure-borne sound from domestic appliances. *Applied Acoustics*, 28:105–117, 1989.

[27] E. Gerretsen. Estimation of air-borne and structure-borne sound transmission from machinery in buildings. *Applied Acoustics*, 40(3):255–265, 1993.

[28] J. Arnold and O. Kornadt. Beschreibung körperschallinduzierter schalldruckpegel mit hilfe von übertragungsfunktionen. In Nabil A. Fouad, editor, *Bauphysik Kalender 2014*, pages 641–663. Wiley-VCH Verlag GmbH, D-69451 Weinheim, Germany, 2014.

[29] C. Hopkins and P. Turner. Field measurement of airborne sound insulation between rooms with non-diffuse sound fields at low frequencies. *Applied Acoustics*, 66:1339–1382, 2005.

[30] ISO 16283-1:2014. Acoustics – field measurement of sound insulation in buildings and of building elements. Part 1: Airborne sound insulation.

[31] C. Hopkins. Revision of international standards on field measurements of airborne, impact and facade sound insulation to form the ISO 16283 series. *Building and Environment*, 92:703–712, 2015.

[32] ISO 16032:2004. Acoustics – measurement of sound pressure level from service equipment in buildings – engineering method.

[33] C. Simmons. Measurement of sound pressure levels at low frequencies in rooms. comparison of available methods and standards with respect to microphone positions. *Acta Acustica united with Acustica*, 85(1):88–100, 1999.

[34] A. R. Mayr and B. M. Gibbs. Point and transfer mobility of point-connected ribbed plates. *Journal of Sound and Vibration*, 330:4798–4812, 2011.